

# Iterative Feedforward Compensation of Hysteresis in Piezo Positioners

Kam K. Leang<sup>†</sup>

Santosh Devasia<sup>‡</sup>

University of Washington, Department of Mechanical Engineering  
Box 352600, Seattle WA, 98195-2600, USA

<sup>†</sup>kleang@u.washington.edu; <sup>‡</sup>devasia@u.washington.edu

**Abstract**—In this article, we prove convergence of an iterative control algorithm to find an input that achieves precise positioning in hysteretic systems. In the analysis, the Preisach hysteresis model is used to characterize the nonlinear behavior of the piezo positioner. We quantify the number of iterations required to achieve a prescribed precision. The method is applied to an experimental piezo system to demonstrate its efficacy, and results show that the positioning error can be reduced to the noise level of the sensor measurement.

## I. INTRODUCTION

Hysteresis effect causes large positioning errors in piezo positioners when they are operated over relatively long ranges [1,2]. Techniques involving feedback and model-based feedforward control have been studied extensively to achieve high-precision positioning, e.g., see Refs. [1-5]. Additionally, researchers have studied the advantages of integrating both techniques to minimize hysteresis, as well as the adverse effects of creep and vibration, e.g., see Refs. [6-8]. Such efforts have managed to reduce the tracking error to 2-3% of the displacement range [6-8]. Although relatively precise positioning is achieved, residual tracking errors may still be large. For example, 2% tracking error over a 50  $\mu\text{m}$  displacement range leaves 1  $\mu\text{m}$  of error, which is certainly larger than the required precision (< 100 nm) of scanning probe microscopy (SPM)-based manufacturing of ultra-small semiconductor devices [9]. Likewise, nanometer-level precision over large positioning ranges is needed in SPM-based studies of cells that vary in size from 100 nm to 50  $\mu\text{m}$  [10]. Therefore, the critical need to achieve high-precision positioning over long ranges motivates our effort to correct for positioning errors due to hysteresis effect.

In this article, we study the iterative control method to find hysteresis-compensating feedforward input. The iterative method can be used in repetitive positioning applications, such as rastering movements [1,2]. The objective is to make use of the information from previous operating trials to improve the response in the next iteration [11,12]. The advantage of this method is that it requires minimal system knowledge; therefore, it reduces the complexity of computing the feedforward input, which traditionally requires inverting nonlinear models [2]. The major contribution of our work is proving convergence of an iterative control algorithm and quantifying the number of iterations required to achieve a prescribed precision. In the analysis, the Preisach hysteresis model is used to characterize the nonlinear behavior in piezo positioners. The hysteresis-compensating feedforward input generated by this approach can be used to further improve the precision of integrated feedback/feedforward schemes, e.g., [7]. The iterative method is applied to an experimental piezo positioning system to demonstrate its effectiveness. Experimental results show that the maximum positioning error can be reduced to less than 0.22% of the total range (25  $\mu\text{m}$ ). This value is below the noise level of the sensor measurements.

The study of the iterative method is presented as follows. First, we formulate the problem in Section II and then briefly discuss the Preisach hysteresis model in Section III. In Section IV, we discuss the properties of the Preisach model in the context of this work and prove convergence of an iterative control algorithm in Section V. Experimental results and a discussion are presented in Section VI. Finally, concluding remarks and acknowledgement follow in Sections VII and VIII, respectively.

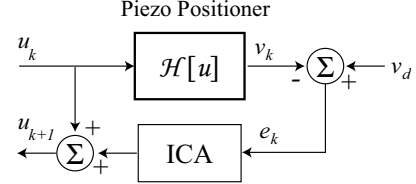


Fig. 1. The iterative control scheme.

## II. PROBLEM FORMULATION

Consider a hysteretic system of the form:

$$v(t) = \mathcal{H}[u](t), \quad (1)$$

where  $u(t) \in \mathbb{R}$  is the input,  $v(t) \in \mathbb{R}$  is the output, and  $\mathcal{H}$  denotes the hysteresis operator. For a given desired trajectory  $v_d(t)$  defined on the finite time interval

$$I \triangleq [t_0, T], \quad (2)$$

the objective is to find an input  $u_d(\cdot)$  by way of the following iterative control algorithm (ICA):

$$\begin{aligned} u_{k+1}(t) &= u_k(t) + \rho[v_d(t) - v_k(t)], \\ &\triangleq u_k(t) + \rho e_k(t), \end{aligned} \quad (3)$$

such that  $v_d(t) = \mathcal{H}[u_d](t)$  for all  $t \in I$ . In Eq. (3),  $\rho$  is a constant (to be determined), and  $v_k(t)$  and  $u_k(t)$  are the output and input for the  $k^{\text{th}}$  operating trial, respectively. Figure 1 shows a block diagram of the iterative control scheme. Our goal is to show that  $u_k \rightarrow u_d$  in the  $\|\cdot\|_\infty$  norm sense, where

$$\|u(\cdot)\|_\infty \triangleq \sup_{t \in I} |u(t)|. \quad (4)$$

Throughout this article, we denote by  $C_m^0(I)$  the set of all continuous monotone functions on  $I$ , and we let  $C_{pm}^0(I)$  represent its piecewise counterpart. We recall that  $C_m^0(I), C_{pm}^0(I) \subset C^0(I)$ . We use the pointwise ordering for functions  $u_1, u_2 \in C^0(I_{a,b})$ , where  $I_{a,b} \triangleq [t_a, t_b]$ , i.e.,  $u_1 \leq u_2$  whenever  $u_1(t) \leq u_2(t)$  for any  $t \in I_{a,b}$ .

**Definition 1: (Incrementally Strictly Increasing Operators)** An operator  $F : C^0(I) \rightarrow C^0(I)$  is called incrementally strictly increasing if, for  $u_1, u_2 \in C^0(I)$  with  $u_1 \leq u_2$ , there exists constants  $\eta_1, \eta_2 > 0$  such that

$$\eta_1(u_2 - u_1) \leq F(u_2) - F(u_1) \leq \eta_2(u_2 - u_1). \quad (5)$$

**Assumption 1:** The incrementally strictly increasing property holds for every closed subinterval  $I_{a,b} \subset I$ .

If a nonlinear operator  $F : C^0(I) \rightarrow C^0(I)$  is incrementally strictly increasing and satisfies Assumption 1, then convergence of the iterative control law Eq. (3) is achieved. This result is summarized as follows.

**Lemma 1:** (Adapted from Venkataraman and Krishnaprasad [13]) Let the nonlinear operator  $F : C^0(I) \rightarrow C^0(I)$  be incrementally strictly

increasing with constants  $\eta_1$  and  $\eta_2$  as defined by Definition 1, and satisfy Assumption 1. Additionally, if the constant

$$0 < \rho \leq \frac{1}{\eta_2}, \quad (6)$$

then

$$\left\| \begin{array}{c} \left(\frac{1}{\rho}u_2 - F(u_2)\right) \\ -\left(\frac{1}{\rho}u_1 - F(u_1)\right) \end{array} \right\|_{\infty} \leq \left(\frac{1}{\rho} - \eta_1\right) \|u_2 - u_1\|_{\infty}, \quad (7)$$

for all  $u_1, u_2 \in C^0(I)$ .

**Proof:** For  $u_1, u_2 \in C^0(I)$  with  $u_1 \leq u_2$ , from Eq. (5) and (6), we find that

$$\begin{aligned} \eta_1(u_2 - u_1) &\leq F(u_2) - F(u_1) \leq \eta_2(u_2 - u_1) \\ &\leq \frac{1}{\rho}(u_2 - u_1). \end{aligned} \quad (8)$$

We rewrite Eq. (8) in the following form:

$$\begin{aligned} 0 &\leq \left(\frac{1}{\rho}u_2 - F(u_2)\right) - \left(\frac{1}{\rho}u_1 - F(u_1)\right) \leq \\ &\quad \left(\frac{1}{\rho} - \eta_1\right)(u_2 - u_1). \end{aligned} \quad (9)$$

Likewise, for  $u_1, u_2 \in C^0(I)$  with  $u_2 \leq u_1$ , we find that

$$\begin{aligned} 0 &\geq \left(\frac{1}{\rho}u_2 - F(u_2)\right) - \left(\frac{1}{\rho}u_1 - F(u_1)\right) \geq \\ &\quad \left(\frac{1}{\rho} - \eta_1\right)(u_2 - u_1). \end{aligned} \quad (10)$$

Applying the  $\|\cdot\|_{\infty}$  norm to Eqs. (9) and (10), we obtain

$$\left\| \begin{array}{c} \left(\frac{1}{\rho}u_2 - F(u_2)\right) \\ -\left(\frac{1}{\rho}u_1 - F(u_1)\right) \end{array} \right\|_{\infty} \leq \left(\frac{1}{\rho} - \eta_1\right) \|u_2 - u_1\|_{\infty}, \quad (11)$$

therefore the assertion holds.

For general  $u_1, u_2 \in C^0(I)$  with  $F$  incrementally strictly increasing and satisfying Assumption 1, we partition the interval  $I$  as follows. First, let the subinterval  $D_1 = \{t \in I | u_1(t) \leq u_2(t)\}$ . The set  $D_1$  is closed. Then Eq. (9) holds for every  $t \in D_1$  (Assumption 1). Let  $\|\cdot\|_{\infty, D_1}$  be the norm on  $C^0(I)$  restricted to  $C_1^0(D_1) = \{u(t) | u(\cdot) \in C^0(I); t \in D_1\}$ . As a result, we find that

$$\left\| \begin{array}{c} \left(\frac{1}{\rho}u_2 - F(u_2)\right) \\ -\left(\frac{1}{\rho}u_1 - F(u_1)\right) \end{array} \right\|_{\infty, D_1} \leq \left(\frac{1}{\rho} - \eta_1\right) \|u_2 - u_1\|_{\infty, D_1}. \quad (12)$$

Second, we let  $D_2 = \{t \in I | u_2(t) \leq u_1(t)\}$ . The set  $D_2$  is also closed. Then Eq. (10) holds for every  $t \in D_2$  (Assumption 1). Let  $\|\cdot\|_{\infty, D_2}$  be the norm on  $C^0(I)$  restricted to  $C_2^0(D_2) = \{u(t) | u(\cdot) \in C^0(I); t \in D_2\}$ . As a result, we find that

$$\left\| \begin{array}{c} \left(\frac{1}{\rho}u_2 - F(u_2)\right) \\ -\left(\frac{1}{\rho}u_1 - F(u_1)\right) \end{array} \right\|_{\infty, D_2} \leq \left(\frac{1}{\rho} - \eta_1\right) \|u_2 - u_1\|_{\infty, D_2}, \quad (13)$$

Now  $I = D_1 \cup D_2$  and  $\|\cdot\|_{\infty} = \max\{\|\cdot\|_{\infty, D_1}, \|\cdot\|_{\infty, D_2}\}$ . Therefore, by Eqs. (12) and (13), we get Eq. (7) for all  $u_1, u_2 \in C^0(I)$ , which completes the proof.  $\blacksquare$

**Theorem 1:** Consider a system of the form  $v(t) = F(u(t))$ . Let the operator  $F : C^0(I) \rightarrow C^0(I)$  be incrementally strictly increasing in any subinterval  $I_{a,b} \subset I$  (Assumption 1). If the constant  $0 < \rho \leq 1/\eta_2$  and  $u_0 \in C^0(I)$ , then the iterative control algorithm Eq. (3) converges, i.e.,

$$\|u_d - u_k\|_{\infty} \leq \gamma^k \|u_d - u_0\|_{\infty}, \quad (14)$$

where  $\gamma < 1$  and  $u_k \rightarrow u_d$ , uniformly in  $t$ , as  $k \rightarrow \infty$ .

**Proof:** To prove the assertion, we show contraction of the input sequence Eq. (3). Subtracting  $u_d(t)$  from both sides of Eq. (3) and substituting  $F(u(t))$  in place of  $v(t)$ , we get

$$\begin{aligned} u_d(t) - u_{k+1}(t) &= u_d(t) - u_k(t) - \rho(v_d(t) - v_k(t)), \\ &= \rho \left( \frac{1}{\rho}u_d(t) - F(u_d(t)) \right) \\ &\quad - \rho \left( \frac{1}{\rho}u_k(t) - F(u_k(t)) \right), \end{aligned} \quad (15)$$

for every  $t \in I$ . Taking the function  $\|\cdot\|_{\infty}$  norm of Eq. (15), we obtain

$$\|u_d - u_{k+1}\|_{\infty} = \rho \left\| \begin{array}{c} \left(\frac{1}{\rho}u_d - F(u_d)\right) \\ -\left(\frac{1}{\rho}u_k - F(u_k)\right) \end{array} \right\|_{\infty}. \quad (16)$$

Since the operator  $F$  is incrementally strictly increasing with constants  $\eta_1 \leq \eta_2$  (Definition 1) and  $0 < \rho \leq 1/\eta_2$ , then by Lemma 1 we obtain

$$\|u_d - u_{k+1}\|_{\infty} \leq \rho \left(\frac{1}{\rho} - \eta_1\right) \|u_d - u_k\|_{\infty} \triangleq \gamma \|u_d - u_k\|_{\infty}, \quad (17)$$

where

$$\gamma = \rho \left(\frac{1}{\rho} - \eta_1\right) = 1 - \rho\eta_1 < 1, \quad (18)$$

because  $0 < \rho\eta_1 \leq 1$ , and Eq. (17) is a contraction. By induction, we find that

$$\|u_d - u_k\|_{\infty} \leq \gamma^k \|u_d - u_0\|_{\infty}, \quad (19)$$

therefore the sequence  $\|u_d - u_k\|_{\infty} \rightarrow 0$  as  $k \rightarrow \infty$ , hence  $u_k$  converges to  $u_d$ , uniformly in  $t$ , which completes the proof.  $\blacksquare$

In the remaining, we check to see if the hysteresis operator  $\mathcal{H}$  satisfies the requirements of Theorem 1 to show convergence of the iterative control algorithm Eq. (3) for hysteretic systems. We start with a brief description of the Preisach hysteresis model.

### III. THE PREISACH HYSTERESIS MODEL

The hysteresis behavior in a piezo positioner is attributed to domain interaction within the material, and such effects lead to nonlinear electromechanical coupling [14]. The Preisach model [15] can be used to model the rate-independent hysteresis effect in piezoelectric materials (e.g., see Ref. [16]), as well as many other hysteretic systems, such as shape memory alloy devices [17]. In the following discussion, the Preisach model will be used to study an iterative control method to compensate for hysteresis in piezo positioners. We briefly discuss the main properties of the model in this section; a detailed discussion of the Preisach model and its properties can be found in Refs. [15,18,19].

The Preisach model is a phenomenological description, whereby the output of a hysteretic system is the net effect of elementary relays, which represent the behavior of individual domains within the material. These domains or relays can assume a value of  $+1$  or  $-1$  depending on the current and future values of the input. The relay operator  $\mathcal{R} : \mathbb{R} \rightarrow \{-1, +1\}$  is defined as [15]:

$$\mathcal{R}_{\alpha, \beta}[u](t) = \begin{cases} +1 & u(t) > \alpha, \\ -1 & u(t) < \beta, \\ \text{unchanged} & \beta \leq u(t) \leq \alpha, \end{cases} \quad (20)$$

where  $u(t)$  is the input. The pair  $(\alpha, \beta)$  in Eq. (20), such that  $\alpha \geq \beta$ , represents the ‘‘up’’ and ‘‘down’’ switching values of the relay, respectively. Figure 2(a) shows an example of an elementary relay (also called Preisach hysteron).

The Preisach model assumes that the output  $v(t)$  of a hysteretic system is an infinite sum of weighted relays  $\mathcal{R}_{\alpha, \beta}$ , each with a unique pair of ‘‘up’’

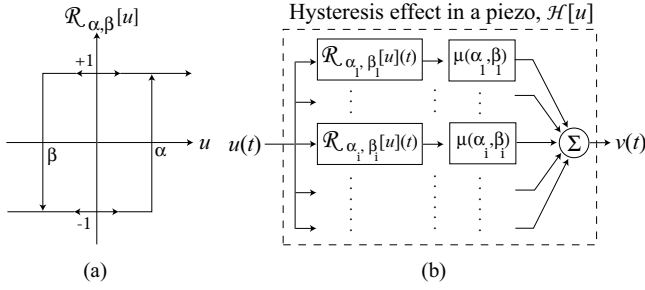


Fig. 2. (a) The elementary relay (Preisach hysteron), and (b) the output  $v(t)$  is the sum of weighted hysterons.

and “down” switching values,  $(\alpha, \beta)$  as shown in Figure 2(b). The output  $v(t)$  is written as

$$v(t) = \mathcal{H}[u](t) = \iint_{\alpha \geq \beta} \mu(\alpha, \beta) \mathcal{R}_{\alpha, \beta}[u](t) d\alpha d\beta, \quad (21)$$

where  $\mu(\alpha, \beta)$  is called the Preisach weighting function, and  $(\alpha, \beta)$  belongs to the Preisach plane  $\mathbf{P}$ , defined as,

$$\mathbf{P} \triangleq \{(\alpha, \beta) | \alpha \geq \beta; \underline{u} \leq \alpha, \beta \leq \bar{u}\}, \quad (22)$$

which happens to be the limiting right-triangle region shown in Fig. 3(a). Equation (22) implies that only relays enclosed in the right-triangle region are affected by the input  $u$  (cf. Fig. 3(a)).

Depending on which relays have been switched to +1 or -1, at time  $t$  the Preisach plane  $\mathbf{P}$  is divided into two regions, i.e.,

$$\mathbf{P}_+(t) \triangleq \{(\alpha, \beta) \in \mathbf{P} : \text{output } \mathcal{R}_{\alpha, \beta}[u](t) = +1\}, \quad (23)$$

$$\mathbf{P}_-(t) \triangleq \{(\alpha, \beta) \in \mathbf{P} : \text{output } \mathcal{R}_{\alpha, \beta}[u](t) = -1\}, \quad (24)$$

with  $\mathbf{P} = \mathbf{P}_+(t) \cup \mathbf{P}_-(t)$ . It follows that the output Eq. (21) can be written in terms of the two sets given by Eq. (23) and (24), i.e.,

$$v(t) = \iint_{\mathbf{P}_+(t)} \mu(\alpha, \beta) d\alpha d\beta - \iint_{\mathbf{P}_-(t)} \mu(\alpha, \beta) d\alpha d\beta. \quad (25)$$

To better understand the Preisach model, we consider its geometric interpretation. Assume at some time  $t_0$  the input  $u(t_0) = \underline{u}$  as shown in Fig. 3(a). Then, from Eq. (20) the output of  $\mathcal{R}_{\alpha, \beta}$ ,  $\forall (\alpha, \beta) \in \mathbf{P}$ , is -1. As

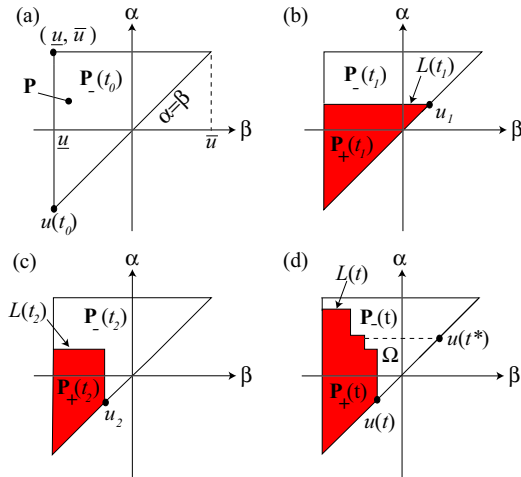


Fig. 3. Behavior of the Preisach boundary.

a result,  $\mathbf{P}_-(t_0) = \mathbf{P}$  and  $\mathbf{P}_+(t_0) = \emptyset$ , otherwise known as the state of “negative saturation”. Next, assume that the input increases monotonically to an arbitrary maximum value  $u_1(t_1)$  at time  $t_1$ . All relays with  $\alpha < u_1(t_1)$  switch to the +1 state, and at time  $t_1$  the boundary separating regions  $\mathbf{P}_-(t_1)$  and  $\mathbf{P}_+(t_1)$  is a horizontal line as shown in Fig. 3(b). We denote this boundary by  $L(t_1)$ . Suppose the input decreases monotonically to an arbitrary value  $u_2(t_2) > \underline{u}$  at time  $t_2$ . As a result relays  $\mathcal{R}_{\alpha, \beta}$  (Eq. (20)), with  $\beta > u_2(t_2)$ , switch to the -1 state, and a vertical line segment  $\beta = u_2(t_2)$  is generated as a part of the boundary separating  $\mathbf{P}_-(t_2)$  and  $\mathbf{P}_+(t_2)$  as shown in Fig. 3(c). Further input reversals generate additional horizontal and vertical links, and in general, at time  $t$  the boundary  $L(t)$  separating regions  $\mathbf{P}_-(t)$  and  $\mathbf{P}_+(t)$  is a nonincreasing staircase function of  $\beta$  as shown in Fig. 3(d) [15]. The last link of the boundary  $L(t)$  intersects the line  $\alpha = \beta$  at point  $(u(t), u(t))$ . This boundary is referred to as the Preisach *memory curve* as it stores the effect of past input. In fact, it captures the effect of past input extremum [15].

Using the fact that  $\mathbf{P} = \mathbf{P}_+(t) \cup \mathbf{P}_-(t)$ , we can express the output Eq. (25) in the following form [17]:

$$v(t) = 2 \iint_{\mathbf{P}_+(t)} \mu(\alpha, \beta) d\alpha d\beta - \iint_{\mathbf{P}} \mu(\alpha, \beta) d\alpha d\beta. \quad (26)$$

Equation (26) implies that the output at time  $t$  can be uniquely determined by knowing the  $\mathbf{P}_+(t)$  region, or equivalently, the boundary  $L(t)$  separating the regions  $\mathbf{P}_+(t)$  and  $\mathbf{P}_-(t)$  (cf. Fig. 3(d)). In fact, the vertices of the boundary  $L(t)$  captures the current input value, the past input extrema, and the order in which they occur [15]. Next, we discuss several properties of the Preisach model relevant to this study.

#### A. Basic Properties of the Preisach Model

##### Assumption 2: (Preisach Model Assumptions)

- We assume the Preisach weighting function is bounded by  $0 < \mu_{\min} \leq \mu(\alpha, \beta) \leq \mu_{\max} < \infty$  and piecewise continuous,  $\forall (\alpha, \beta) \in \mathbf{P}$ .
- We assume the input  $u \in [\underline{u}, \bar{u}]$ .

We denote by  $L_0$  at time  $t_0$  the *initial memory curve* and it represents the initial state of the Preisach operator. Below, we summarize some basic properties of the Preisach operator, see, e.g., [18].

Let Assumption 2 be satisfied and  $L_0$  be some initial memory curve:

**Property 1: (Strong Continuity)**  $\mathcal{H} : C^0(I) \rightarrow C^0(I)$  is strongly continuous (in the sup norm) (e.g., see Ref. [18], Section 3).

**Property 2: (Piecewise Monotonicity)** The output  $v \in C_m^0(I)$  strictly increasing (decreasing) if and only if  $u \in C_m^0(I)$  strictly increasing (decreasing) (e.g., see Ref. [18], Section 5).

**Proposition 1:** Suppose the input  $u(t)$ , at time instant  $t$ , is changed monotonically to  $u(t^*)$ , at time instant  $t^*$ . As a result the boundary sweeps out an area  $\Omega$ , which is illustrated in Fig. 3(d) for a monotonically increasing input, for example. Then, the output variation associated with this monotonic change in input is

$$v(t) - v(t^*) = 2 \text{sgn}[u(t) - u(t^*)] \iint_{\Omega} \mu(\alpha, \beta) d\alpha d\beta. \quad (27)$$

**Proof:** The proof follows directly from the construction of the Preisach model (e.g., see Ref. [17], Proposition 2.1). ■

#### IV. PROPERTIES OF THE HYSTERESIS OPERATOR ON A BRANCH

In this section we verify that the hysteresis operator satisfies the conditions of Lemma 1, therefore allowing the direct use of Theorem 1. Namely, we show that if certain conditions are satisfied, the Preisach hysteresis operator  $\mathcal{H}$  is incrementally strictly increasing for every subinterval  $I_{a,b} \triangleq [t_a, t_b] \subset I \triangleq [t_0, T]$ .

**Assumption 3:** The desired trajectory  $v_d \in C^0(I)$  is given and increasing on  $I$ .

**Remark 1:** By the Preisach Property 1 and Property 2,  $u_d \in C^0(I)$  is increasing. The following results are developed for  $v_d$  satisfying Assumption 3; however, the discussion also applies to the decreasing case.

**Definition 2: (Branch)** Let  $L_0$  be some initial memory curve and  $u \in C_m^0(I)$  be increasing (decreasing) in time, then we say the pair  $(u, \mathcal{H}[u])$  belongs to the branch  $\mathcal{B}_\uparrow(L_0)$  ( $\mathcal{B}_\downarrow(L_0)$ ). A branch is an increasing function of  $u$  by the Preisach Property 2.

Examples of three different branches with initial memory curves  $L_0$ ,  $\tilde{L}_0$ , and  $L_0^*$  are shown in Fig. 4(a).

**Definition 3: (Turn-around Point)** We call a turn-around point the location on the  $u$ - $v$  plane where the input  $u$  changes from increasing to decreasing in time or vice versa, e.g., see Figs. 4(a) and (b).

In the following lemma, we show the property of a branch for the Preisach hysteresis operator  $\mathcal{H}$ .

**Lemma 2: (Property of a Branch)** Let Assumption 2 hold and  $L_0$  be an initial memory curve. Given  $u_1, u_2 \in C_m^0(I)$  such that  $(u_1, \mathcal{H}[u_1])$  and  $(u_2, \mathcal{H}[u_2])$  belong on a single branch  $\mathcal{B}_\uparrow[\cdot, L_0]$  and for any  $t_1, t_2 \in I$  such that  $u_1(t_1) \leq u_2(t_2)$ , then

$$\begin{aligned} \mu_{\min}(u_2(t_2) - u_1(t_1))^2 &\leq \mathcal{H}[u_2](t_2) - \mathcal{H}[u_1](t_1) \\ &\leq 2\mu_{\max}(\bar{u} - \underline{u})(u_2(t_2) - u_1(t_1)). \end{aligned} \quad (28)$$

**Proof:** The pair  $(u_1, \mathcal{H}[u_1])$  and  $(u_2, \mathcal{H}[u_2])$  belonging to a single branch  $\mathcal{B}_\uparrow[\cdot, L_0]$  implies that  $u_1, u_2 \in C_m^0(I)$  are increasing (Definition 2). If  $u_1(t_1) \leq u_2(t_2)$ , then the Preisach plane is partitioned as shown in Fig. 4(c). The difference in output  $\mathcal{H}[u_2](t_2) - \mathcal{H}[u_1](t_1)$  is related to the difference in the regions  $\mathbf{P}_{2+}(t_2)$  and  $\mathbf{P}_{1+}(t_1)$ . Let  $\hat{\Omega}$  represent the difference in the regions  $\mathbf{P}_{2+}(t_2)$  and  $\mathbf{P}_{1+}(t_1)$  as shown in Fig. 4(c). By Proposition 1, we can write

$$\begin{aligned} \mathcal{H}[u_2](t_2) - \mathcal{H}[u_1](t_1) &= 2 \iint_{\hat{\Omega}} \mu(\alpha, \beta) d\alpha d\beta, \\ &\geq 2\mu_{\min} \iint_{\hat{\Omega}} d\alpha d\beta, \\ &\geq 2\mu_{\min} \left[ \frac{1}{2}(u_2(t_2) - u_1(t_1))^2 \right], \\ &\geq \mu_{\min}(u_2(t_2) - u_1(t_1))^2, \end{aligned} \quad (29)$$

for any  $t_1, t_2 \in I$ . Similarly, the largest region  $\hat{\Omega}$  is shown in Fig. 4(d),

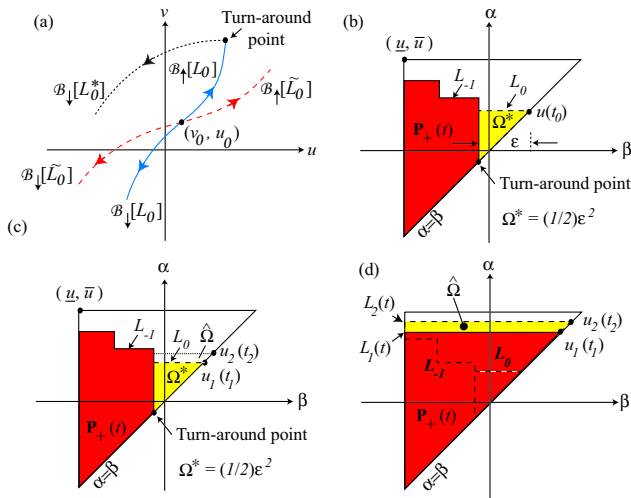


Fig. 4. (a) Branches; (b)-(c) Behavior of memory curve with change in  $u$ .

which gives us

$$\begin{aligned} \mathcal{H}[u_2](t_2) - \mathcal{H}[u_1](t_1) &\leq 2\mu_{\max} \left[ (\bar{u} - \underline{u})(u_2(t_2) - u_1(t_1)) \right. \\ &\quad \left. - \frac{1}{2}(u_2(t_2) - u_1(t_1))^2 \right], \\ &\leq 2\mu_{\max}(\bar{u} - \underline{u})(u_2(t_2) - u_1(t_1)), \end{aligned} \quad (30)$$

for any  $t_1, t_2 \in I$ . Therefore, Eqs. (29) and (30) leads to Eq. (28), which completes the proof. ■

### A. Incrementally Strictly Increasing Preisach Operator

**Assumption 4:** We assume that the last link of the initial memory curve  $L_0$  is  $\epsilon > 0$  away from a turn-around point, for example, as shown in Fig. 4(b), where  $L_{-1}$  represents the memory curve with the last link at a turn-around point. The area swept by the  $\epsilon$  change is given by the region  $\Omega^* = (1/2)\epsilon^2$  (cf. Fig. 4(b)).

**Corollary 1:** Let Assumption 2 hold and  $L_0$  be an initial memory curve satisfying Assumption 4. Given  $u_1, u_2 \in C_m^0(I)$  such that the pair  $(u_2, \mathcal{H}[u_1])$  and  $(u_2, \mathcal{H}[u_2])$  belong on a single branch  $\mathcal{B}_\uparrow[\cdot, L_0]$ , then the Preisach hysteresis operator  $\mathcal{H}$  is incrementally strictly increasing on any closed subinterval  $I_{a,b} \subset I$ , i.e., if  $u_1$  and  $u_2$  are restricted to the subinterval  $I_{a,b}$  with  $u_1|_{t \in I_{a,b}} \leq u_2|_{t \in I_{a,b}}$ , then

$$\begin{aligned} \eta_1(u_2|_{t \in I_{a,b}} - u_1|_{t \in I_{a,b}}) &\leq (\mathcal{H}[u_2]|_{t \in I_{a,b}} - \mathcal{H}[u_1]|_{t \in I_{a,b}}) \\ &\leq \eta_2(u_2|_{t \in I_{a,b}} - u_1|_{t \in I_{a,b}}), \end{aligned} \quad (31)$$

where  $\eta_1 = 2\mu_{\min}\epsilon > 0$  and  $\eta_2 = 2\mu_{\max}(\bar{u} - \underline{u})$ .

**Proof:** Since  $(u_1, \mathcal{H}[u_1]), (u_2, \mathcal{H}[u_2]) \in \mathcal{B}_\uparrow[\cdot, L_0]$ , then given any  $t_1, t_2 \in I_{a,b} \subset I$  such that  $u_2(t_2) \leq u_1(t_1)$ , then by Lemma 2, Eq. (28) holds. Furthermore, by Assumption 4, the region  $\Omega^* = (1/2)\epsilon^2 > 0$  as shown in Figs. 4(b) and (c). This implies that

$$\begin{aligned} \mathcal{H}[u_2](t_2) - \mathcal{H}[u_1](t_1) &\geq 2\mu_{\min} \iint_{\hat{\Omega}} d\alpha d\beta, \\ &\geq 2\mu_{\min} \left[ \epsilon(u_2(t_2) - u_1(t_1)) \right. \\ &\quad \left. + \frac{1}{2}(u_2(t_2) - u_1(t_1))^2 \right], \\ &\geq 2\mu_{\min}\epsilon(u_2(t_2) - u_1(t_1)), \\ &\triangleq \eta_1(u_2(t_2) - u_1(t_1)), \end{aligned} \quad (32)$$

for any  $t_1, t_2 \in I_{a,b} \subset I$ . Similarly, the largest region  $\hat{\Omega}$  is shown in Fig. 4(d), and Eq. (30) in Lemma 2 holds for any  $t_1, t_2 \in I_{a,b} \subset I$ . Therefore, the claim is true for any subinterval  $I_{a,b} \subset I$  as required, which completes the proof. ■

**Remark 2:** The pair  $(u, \mathcal{H}[u])$  does not have to belong to a branch  $\mathcal{B}_\uparrow[u, L_0]$  for the Preisach operator  $\mathcal{H}$  to be incrementally strictly increasing for all subintervals  $I_{a,b} \subset I$ . In fact, given an initial boundary  $L_0$  that satisfies Assumption 4 and  $u_1, u_2 \in C^0(I)$  with  $u_1 \leq u_2$ , Assumption 1 is satisfied.

**Remark 3:** On the other hand, for general  $u_1, u_2 \in C^0(I)$ , the Preisach operator does not satisfy Assumption 1, i.e.,  $\mathcal{H}$  is not incrementally strictly increasing on all subintervals of  $I_{a,b} \subset I$ . To illustrate, consider Fig. 5, where (a) plots the input versus time, (b) plots the output versus time, and (c) plots a typical hysteresis curve for  $u_1, u_2 \in C^0(I = [t_0, T])$ . For  $D_1 = [t_0, t_1]$ ,  $u_1(t) \leq u_2(t)$  for every  $t \in D_1$ , and it can be shown that the operator  $\mathcal{H}$  is incrementally strictly increasing (cf. Definition 1 and Eq. (5)). However, Assumption 1 fails for  $D_3 = [t_2, t_3]$  because  $u_2|_{t \in D_3} \leq u_1|_{t \in D_3}$ , but  $\mathcal{H}[u_1]|_{t \in D_3} \leq \mathcal{H}[u_2]|_{t \in D_3}$ .

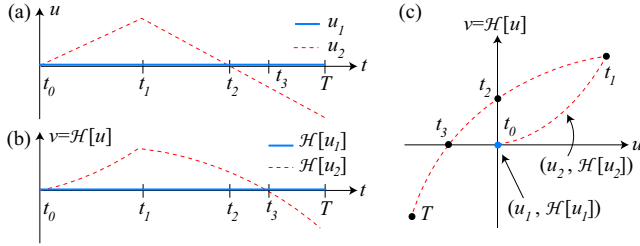


Fig. 5. (a) Input vs. time; (b) output vs. time; and (c) hysteresis curve.

## V. ITERATIVE FEEDFORWARD HYSTERESIS COMPENSATION

The discussion in Remark 3 leads to the following approach to prove convergence of the iterative control algorithm Eq. (3). We notice that Assumption 1 is satisfied if  $(u, \mathcal{H}[u])$  belongs to a branch  $\mathcal{B}[u, L_0]$ , where  $L_0$  satisfies Assumption 4. Then this implies that the input  $u$  be monotonic on  $I$ . Consequently,  $u$  monotonic implies that the output be monotonic on  $I$  (Preisach Property 2). By this observation, if the desired trajectory  $v_d(t)$  is chosen to be monotonic on  $I$ , then  $(u, \mathcal{H}[u])$  belongs on a branch, and Assumption 1 is satisfied, therefore convergence of iterative control algorithm Eq. (3) is achieved. This result is shown in the following. To show convergence for a general  $v_d$ , our approach is to partition it into monotonic sections as shown in Fig. 6 and apply the results to each section individually, until convergence for all sections of the desired trajectory is achieved. We start by showing that the sequence  $u_k$  generated by Eq. (3) is monotonic for all  $k$  if  $v_d$  is monotonic, hence  $(u_k, \mathcal{H}[u_k])$  belongs on a single branch  $\mathcal{B}[u, L_0]$  and Assumption 1 holds.

**Definition 4: (Initial Input)** For a given initial memory curve  $L_0$  at time  $t_0$ , we call  $u(t_0)$  the input value at the intersection of the last link of  $L_0$  with the line  $\alpha = \beta$  in the Preisach plane, e.g., see Figs. 3(d) and 4(b).

**Lemma 3: (Input Monotonicity)** Let the conditions of Lemma 2 be satisfied. Let  $v_d(t)$  be increasing (decreasing) and  $u_0(t) = u(t_0)$  for all  $t \in I = [t_0, T]$  as defined in Definition 4. If  $0 < \rho \leq 1/\eta_2$ , then the input sequence generated by Eq. (3) is increasing (decreasing) on  $I$  for  $k = 0, 1, 2, \dots$ .

**Proof:** We prove the increasing case; the decreasing case is similar and omitted for brevity. Let  $k = 0$ , then by Eq. (3), for any  $t_1 < t_2 \in I$ , we have

$$\begin{aligned} u_1(t_2) - u_1(t_1) &= u_0(t_2) + \rho(\mathcal{H}[u_d](t_2) - \mathcal{H}[u_0](t_2)) \\ &\quad - u_0(t_1) - \rho(\mathcal{H}[u_d](t_1) - \mathcal{H}[u_0](t_1)). \end{aligned} \quad (33)$$

Substituting the terms in Eq. (33) with the result of Lemma 2, we obtain

$$\begin{aligned} u_1(t_2) - u_1(t_1) &\geq (1 - \rho\mu_{\min}(u_0(t_2) - u_0(t_1))) \\ &\quad \times (u_0(t_2) - u_0(t_1)) \\ &\quad + \rho\eta_2(u_d(t_2) - u_d(t_1)) > 0, \end{aligned} \quad (34)$$

because  $u_0$  and  $u_d$  are increasing on  $I$  (Preisach Property 2), and

$$0 \leq \rho\mu_{\min}(u_0(t_2) - u_0(t_1)) \leq \rho\mu_{\min}(\bar{u} - \underline{u}) \leq \rho\eta_2 \leq 1. \quad (35)$$

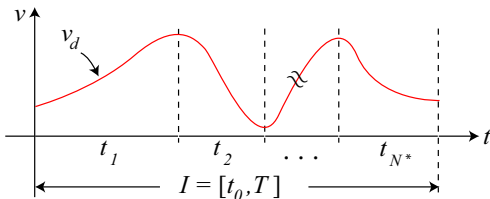


Fig. 6. Monotonic partitioning of the desired output.

Also note that by induction,

$$\begin{aligned} u_{k+1}(t_2) - u_{k+1}(t_1) &\geq (1 - \rho\mu_{\min}(u_k(t_2) - u_k(t_1))) \\ &\quad \times (u_k(t_2) - u_k(t_1)) \\ &\quad + \rho\eta_2(u_d(t_2) - u_d(t_1)) > 0, \end{aligned} \quad (36)$$

because  $u_k$  and  $u_d$  are increasing on  $I$  (Preisach Property 2), and Eq. (35) holds for  $k = 0, 1, 2, \dots$ , which completes the proof. ■

**Theorem 2:** Consider a hysteretic system of the form  $v(t) = \mathcal{H}[u](t)$ . Let the Preisach hysteresis operator  $\mathcal{H}$  satisfy Assumptions 1–4 where  $0 < \rho \leq 1/\eta_2$  and  $u_0(t) = u(t_0)$  for all  $t \in I$ . Then the iterative control algorithm Eq. (3) converges, i.e.,

$$\|u_d - u_k\|_\infty \leq \gamma^k \|u_d - u_0\|_\infty, \quad (37)$$

where  $\gamma < 1$ , hence  $u_k \rightarrow u_d$ , uniformly in  $t$ , as  $k \rightarrow \infty$ .

**Proof:** With Assumptions 1–4 satisfied, the proof is identical to the proof of Theorem 1. ■

**Remark 4:** Lemmas 2 and 3, Corollary 1, and Theorem 2 also apply to the case when  $(u, \mathcal{H}[u]) \in \mathcal{B}_1[u, L_0]$ , i.e., when  $u, v \in C^0(I)$  are decreasing. The proofs follow similar procedures as discussed in the previous sections.

Suppose a precision  $\delta > 0$  is specified for the input sequence. The number of iterations required to achieve the precision  $\delta$  is determined as follows. By Eq. (37), we write

$$\begin{aligned} \|\Delta u_k\|_\infty &\triangleq \|u_d - u_k\|_\infty \leq \gamma^k \|u_d - u_0\|_\infty \\ &\leq \gamma^{\mathcal{K}} (\bar{u} - \underline{u}) < \delta, \end{aligned} \quad (38)$$

where  $\gamma = \rho(\frac{1}{\rho} - \eta_1)$  and  $0 < \rho \leq 1/\eta_2$ . Solving for the required number of iterations  $\mathcal{K}$  in terms of  $\delta$  using Eq. (38), we obtain

$$k > \mathcal{K} = \frac{\ln(K_1\delta)}{\ln(K_2)}, \quad (39)$$

where

$$\begin{aligned} K_1 &= \frac{1}{\bar{u} - \underline{u}}, \\ K_2 &= 1 - 2\rho\mu_{\min}\varepsilon, \end{aligned} \quad (40)$$

and the value  $\varepsilon > 0$  is described in Assumption 4.

Now we discuss the extension of the results of Theorem 2 for a general desired trajectory. First, we say that  $\Lambda(v) = \{t_i\}_{0 \leq i \leq N}$ ,  $t_0 = t_0 < t_1 < \dots < t_N = T$ , is a *monotonicity partition* for  $v: I \rightarrow \mathbb{R}$ , if  $v$  is monotone on all subintervals  $[t_i, t_{i+1}] \subset I$  (e.g., see Ref. [19], Definition 2.2.2). Second, by  $N_m(\Lambda(v))$  we denote the number of monotonicity intervals in the monotonicity partition of  $v$ .

**Proposition 2:** Consider a hysteretic system of the form  $v(t) = \mathcal{H}[u](t)$ . Let  $v_d(t) \in C^0(I)$  be given with the number of monotonicity intervals equal to  $N_m(v_d) = N^*$  and for given  $\delta > 0$ , the total number of iterations  $\mathcal{K}^*$ , such that  $\|\Delta u_k\|_\infty < \delta$  whenever  $k > \mathcal{K}^*$  is

$$\mathcal{K}^* = N^* \times \mathcal{K}, \quad (42)$$

where  $\mathcal{K}$  is given by Eq. (39).

**Proof: (Outline)** For a given  $v_d \in C^0(I)$ , we form the monotonicity partition  $\Lambda(v_d)$  of the desired trajectory  $v_d$ . Given  $\delta > 0$ , we apply Theorem 2 to the first monotonic section of  $v_d$ , and the number of iterations required to achieve the precision  $\delta$  is given by Eq. (39). After  $k > \mathcal{K}$  number of iterations, the input  $u_k(t)$  and output  $v_k(t)$  for  $t \in [t_0, t_1]$  are chosen as the desired input-output pair for the first monotonic section. At time  $t_1$ , the memory curve achieved by the input  $u_k(t)$  for  $t \in [t_0, t_1]$  is chosen as the initial memory curve  $L_0$  for the next monotonic section of  $v_d$ , i.e.,  $v_d(t)$  for  $t \in [t_1, t_2]$ . Then, Theorem 2 is applied again, which yields another  $\mathcal{K}$  number of iterations required to achieve the precision of  $\delta$ . This process is repeated  $N^*$ -times and we find that  $\mathcal{K}^* = N^* \times \mathcal{K}$ . ■

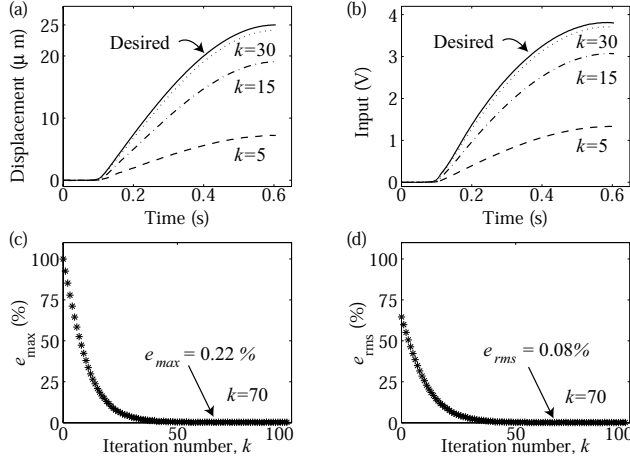


Fig. 7. Experimental results: (a) displacement vs. time, (b) input vs. time, (c)  $e_{max}$  vs.  $k$ , and (d)  $e_{rms}$  vs.  $k$ .

## VI. EXPERIMENTAL RESULTS AND DISCUSSION

The iterative method was applied to an experimental piezo positioning system to demonstrate high-precision positioning over long ranges (the experimental system is described in Ref. [7]). The constant  $\rho$  in Eq. (3) was chosen sufficiently small, e.g.,  $\rho = 0.30$ . At each trial, the piezo positioner was “initialized” (Assumption 4) by applying a sinusoidal input whose amplitude slowly decays to zero from the value  $\max\{|\bar{u}|, |\underline{u}|\} = 5.0$  V. As a result, at the initial time  $t_0$ ,  $u(t_0) = 0$  and  $v(t_0) = 0$ . Therefore at the initial trial, the input was selected as  $u_0(t) = 0$ , hence  $v_0(t) = 0$  for all  $t \in [t_0, T]$ . We applied the iterative input law Eq. (3) to track: (a) a monotonically increasing trajectory from zero to  $25 \mu\text{m}$ , and (b) a  $0.5$  Hz,  $25 \mu\text{m}$  amplitude sinusoidal trajectory. The experimental results are shown in Figs. 7 and 8.

The results in Fig. 7 show that precision tracking of a monotonically increasing trajectory can be achieved. In fact, after 70 iterations, the maximum error  $e_{max}$  and the root-mean-square error  $e_{rms}$  as a percentage of the total displacement range ( $25 \mu\text{m}$ ), defined as

$$e_{max} = \frac{\max |e_k(\cdot)|}{25 \mu\text{m}} \times 100\%, \quad e_{rms} = \frac{\sqrt{\frac{1}{T} \int_{t_0}^T |e_k(t)|^2 dt}}{25 \mu\text{m}} \times 100\%,$$

reduces to 0.22% and 0.08%, respectively. As the results suggest in Figs. 7(c) and (d),  $e_{max}$  and  $e_{rms}$  decay rapidly as the iteration number  $k$  increases. In terms of precision,  $e_{max} = 0.22\%$  corresponds to  $55 \text{ nm}$ , or equivalently, the measured sensor voltage of  $2.70 \text{ mV}$ . In comparison, the amplitude of the measured sensor noise is approximately  $\pm 3.00 \text{ mV}$ .

Figure 8 shows the results of the iterative method applied to track a sinusoidal trajectory (with more than one monotonic section). Convergence is achieved as shown in Fig. 8(a). The hysteresis effect in the experimental system can be observed by plotting the desired displacement versus the feedforward input at the  $k = 100$  trial as shown in Fig. 8(b). The maximum output hysteresis measures 12.26% of the total displacement range ( $50 \mu\text{m}$ ). Thus, the iterative control method finds hysteresis-compensating input, and therefore achieves high-precision positioning.

## VII. CONCLUSIONS

In conclusion, we studied the convergence of an iterative control algorithm for hysteretic systems. The method was applied to find hysteresis-compensating feedforward input, and experimental results demonstrate that the positioning error can be reduced to the noise level of the sensor measurements.

## VIII. ACKNOWLEDGEMENT

This work was supported by the National Science Foundation under Grant NSF-CMS 0301787.

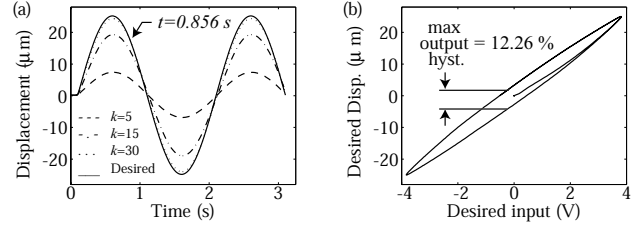


Fig. 8. Experimental results: (a) displacement vs. time and (b) hysteresis curve.

## IX. REFERENCES

- [1] R. C. Barrett and C. F. Quate. Optical scan-correction system applied to atomic force microscopy. *Rev. Sci. Instrum.*, 62(6):1393–1399, 1991.
- [2] D. Croft, G. Shed, and S. Devasia. Creep, hysteresis, and vibration compensation for piezoactuators: atomic force microscopy application. *ASME J. Dyn. Syst., Meas., and Control*, 123:35–43, March 2001.
- [3] Y. Okazaki. A micro-positioning tool post using a piezoelectric actuator for diamond turning machines. *Precision Engineering*, 12(3):151–156, July 1990.
- [4] H. Janocha and K. Kuhnen. Real-time compensation of hysteresis and creep in piezoelectric actuators. *Sensors and actuators A*, 79:83–89, 2000.
- [5] S. Salapaka, A. Sebastin, J. P. Cleveland, and M. V. Salapaka. High bandwidth nano-positioner: a robust control approach. *Rev. Sci. Instr.*, 73(9):3232–3241, 2002.
- [6] P. Ge and M. Jouaneh. Tracking control of a piezoceramic actuator. *IEEE Trans. Contr. Syst. Tech.*, 4(3):209–216, 1996.
- [7] K. K. Leang and S. Devasia. Hysteresis, creep, and vibration compensation for piezoactuators: feedback and feedforward control. In *The 2<sup>nd</sup> IFAC Conference on Mechatronic Systems*, pages 283–289, Berkeley, CA, December 2002.
- [8] M.-S. Tsai and J.-S. Chen. Robust tracking control of a piezoactuator using a new approximate hysteresis model. *ASME J. Dyn. Syst., Meas., Control*, 125:96–102, March 2003.
- [9] C. F. Quate. Scanning probes as a lithography tool for nanostructures. *Surface Science*, 386:259–264, 1997.
- [10] P. P. Lehenkari, G. T. Charras, A. Nykänen, and M. A. Horton. Adapting atomic force microscopy for cell biology. *Ultramicroscopy*, 82:289–295, 2000.
- [11] S. Arimoto, S. Kawamura, and F. Miyazaki. Bettering operation of robots by learning. *J. of Robotic Systems*, 1(2):123–140, 1984.
- [12] K. L. Moore. *Iterative learning control for deterministic systems*. Springer-Verlag, New York, 1993.
- [13] R. Venkataraman and P. S. Krishnaprasad. Approximate inversion of hysteresis: theory and numerical results. In *Proc. 39th IEEE Conf. on Decision and Control*, pages 4448–4454, Sydney, Australia, December 2000.
- [14] O. Boser. Statistical theory of hysteresis in ferroelectric materials. *J. Appl. Phys.*, 62(4):1344–1348, August 1987.
- [15] I. D. Mayergoyz. *Mathematical models of hysteresis*. Springer-Verlag, New York, 1991.
- [16] D. Hughes and J. T. Wen. Preisach modeling of piezoceramic and shape memory alloy hysteresis. *Smart Mater. Struct.*, 6:287–300, 1997.
- [17] R. B. Gorbet, D. W. L. Wang, and K. A. Morris. Preisach model identification of a two-wire SMA actuator. In *Proc. IEEE Int. Conf. on Robotics and Automation*, pages 2161–2167, Leuven, Belgium, May 1998.
- [18] Martin Brokate and Augusto Visintin. Properties of the Preisach model for hysteresis. *Journal fur die reine und angewandte Mathematik*, 402:1–40, 1989.
- [19] Martin Brokate and Jurgen Sprekels. *Hysteresis and phase transitions*. Springer, New York, 1996.